PERGAMON

International Journal of Heat and Mass Transfer 44 (2001) 1019–1030

International Journal of HEAT and MASS TRANSFER

www.elsevier.com/locate/ijhmt

Heat transfer measurements in transitional boundary layers

R. Schook *, H.C. de Lange, A.A. van Steenhoven

Faculty of Mechanical Engineering, Eindhoven University of Technology, P.O. Box 513, 5600 MB Eindhoven, Netherlands

Received 13 September 1999; received in revised form 27 March 2000

Abstract

High velocity boundary layer transition experiments are performed in a Ludwieg tube set-up. At a Mach number of 0.36, the transition is studied by using several turbulence generating grids. These grids cause turbulence levels varying from 0.25% to 3.5%. It is found that, depending on the turbulence level, different intermittency distributions should be used to describe the transition zone well. For low turbulence levels, the Narasimha and the Johnson models, which are based on turbulent spots, show good agreement with the measurements. For intermediate levels, the front part of the transition zone follows a distribution which is described by turbulent spots which decrease in size. In these cases, the latter part of transition also shows agreement with the Narasimha and Johnson models. A major difference with the 'classical' intermittency distributions is obtained for high turbulence levels. Assuming that for these levels non-growing turbulent spots are initiated in the whole transition zone, an exponential intermittency is derived. In the measurements these distributions indeed are found.

Keywords: Boundary layer; Heat transfer; Turbines

1. Introduction

The boundary layer heat transfer increases significantly when laminar to turbulent transition occurs. Especially, in turbomachines, where hot gases from the combustion chamber force an enormous heat flux to the turbine blades, it is of major importance to know this heat transfer exactly. Almost half the area of the turbine blades is covered by the transition zone. Due to these high heat fluxes, it is very important to know the influence of several parameters on the transition because a delay of the start, or increase of the transition length, has a large effect on the total heat transfer.

Transition is influenced by the turbulence level, turbulence length scale, Reynolds number and pressure gradient. There are also effects of compressibility and surface curvature. An overview of parameters can be found in [1–3].

When transition starts it is assumed that turbulent spots are initiated in the laminar boundary layer. These spots were discovered by Emmons [4] in a water tunnel. It is supposed that a turbulent spot is a local area of turbulence. Most transition models which are used nowadays are based on these turbulent spots. Dhawan and Narasimha [5] argued that the spots are initiated with infinitesimal small size in a narrow area around the transition start. The spots convect in streamwise direction with a mean velocity which is less than the main flow velocity. The leading edge travels faster than the trailing edge and so the turbulent spot grows lengthwise while moving in downstream direction. Furthermore, the spots appear to remain in the same shape so they also grow laterally. At a certain point, the spots start to merge until the flow is completely turbulent. This is said to be the end of transition. Narasimha [6] derived an analytical solution for the intermittency distribution by assuming that all spots originate from one streamwise position. Johnson and Fashifar [7] assumed a distributed breakdown of infinitesimal small turbulent spots and obtained good results for low turbulence level transition experiments.

In general, a distinction between natural and bypass transition should be made [8]. For low disturbance levels in the main flow Tollmien–Schlichting waves are initiated at a certain Reynolds number. These waves grow

* Corresponding author. Tel.: +31-40-247-2320; fax: +31-40-243-3445.

E-mail address: r.schook@wtb.tue.nl (R. Schook).

0017-9310/01/$ - see front matter
PII: S0017-9310(00)00161-7

Nomenclature

a	decay parameter
c	specific heat
$F(\gamma)$	transformation function
J	constant
k	thermal conductivity
m	spot formation rate (m^{-2})
M	Mach number
n	spot formation rate (m^{-1} s^{-1})
$\hat{n}$	dimensionless spot formation rate
N	number of spots
Nu	Nusselt number
p	pressure
Pr	Prandtl number
q''	heat flux
q_l	laminar heat flux
q_t	turbulent heat flux
$\overline{q}$	averaged measured heat flux
R	electrical resistance
Re	Reynolds number
Re_u	unit Reynolds number (m^{-1})
Re_x	local Reynolds number
Re_{tr}	transition start Reynolds number
Re_θ	momentum thickness Reynolds number
s	transformation coefficient
St	Stanton number
t	time
T	temperature
T_r	recovery temperature
Tu	turbulence level
U	mainstream velocity
w	spot size
x	streamwise distance
z	coordinate perpendicular to surface

Greek symbols

α	temperature resistance coefficient
β	spot half spreading angle
γ	intermittency
γ	specific heat ratio
v	kinematic viscosity
ρ	density
σ	turbulent spot propagation parameter
θ	boundary layer momentum thickness

in amplitude and three-dimensional waves start to develop. Further downstream, the first turbulent spots occur until transition is completed. This scenario is called natural transition. However, for higher turbulence levels the Tollmien–Schlichting and three-dimensional waves do not occur. The disturbances in the main flow enter the boundary layer and turbulent spots are initiated immediately. This is called bypass transition (bypassing to transition in the natural mode). Mayle [3] argued that turbulence levels above 0.4% cause bypass transition.

Most experiments on transition are performed in low speed wind tunnels [9–11]. In most cases, hot-wire experiments are used to determine transition characteristics. Velocity profiles in the boundary layer are measured from which the skin friction coefficient is determined. This method only works at low main stream velocities, when the boundary layer is thick enough to obtain sufficient data points. From the thus determined friction coefficient, the intermittency can be determined as the fraction of the increase of friction relative to the increase of friction that would occur in a fully turbulent boundary layer. Another possibility is to analyse the hot-wire signal measured close to the wall. In the transition zone, this signal shows an intermittent behaviour between 'laminar' and 'turbulent' as a function of time. From this, the intermittency is calculated by evaluating the fraction of time the flow is turbulent.

At higher main stream velocities, heat transfer experiments are more convenient to use. This method has the additional advantage of directly determining the transitional data that are of direct interest for gas turbine purposes. Furthermore, heat transfer techniques do not disturb the boundary layer.

Transitional heat flux experiments in transient facilities can be found in literature. High velocities are obtained for a short time by using, for example, an isentropic light piston tunnel (ILPT) [12] or a Ludwieg tube with isentropic compression heating (LICH) [13]. These measurements are performed in low turbulence flows where naturally occurring spot properties are determined. Bypass transition experiments on instrumented blades also can be found [14]. They showed that the heat transfer on a turbine blade indeed increases significantly when laminar to turbulent transition occurs.

High velocity measurements at high turbulence levels on a flat plate are scarce. Blair [11] conducted a large series of experiments with turbulence levels up to 7%. However, these experiments were performed at a relatively low velocity (30 m/s).

This paper describes measurements to obtain transitional data at high (subsonic) velocities. The measurements are performed in a Ludwieg tube set-up. In this set-up well-defined high velocity flows can be generated. Measurements are performed in a wide range of flow parameters which are important for turbomachinery design.

First, the experimental set-up is described. Second, hot-wire and heat transfer measurements are presented. For the latter, a thin film technique is used. From these

results the transitional data are obtained. It is shown that for low turbulence levels the results agree very well with literature. However, for higher turbulence levels, the traditional transition models based on turbulent spots had to be modified. Also, some new ideas about pre-transition are presented. The new model thus derived gives good agreement with the data obtained.

2. Experimental set-up

The experiments are performed in a Ludwieg tube. Hogendoorn [15] showed that it is possible to obtain well-defined flow conditions in this set-up. A large range of flow conditions is covered in a Ludwieg tube. For example, the Mach number can reach values up to 0.55 and the unit Reynolds number ($Re_u = U/\nu$) can reach values up to 5×10^6 m^{-1}. The experimental facility consists of a tube connected to a test section. This section contains a flat plate with thin film sensors for measuring the surface temperature. Just above the plate, a hot-wire can be mounted. The side wall of the section contains a pressure gauge. Upstream of the leading edge, several turbulence generating grids can be positioned. A schematic view of the experimental set-up is given in Fig. 1.

The test section is connected to a dump tank via a diaphragm and a choking orifice. Prior to an experiment the pressure in the dump tank is brought to 300 N m^{-2}, while the pressure in the tube and the test section is set to a value which is less than or equal to the ambient pressure. When the membrane is ruptured, by an electrical pulse, an expansion wave travels from the dump tank towards the end of the tube and vice versa. During this time, which is approximately 40 ms, a constant flow along the sensor plate is obtained. Due to the expansion, the gas temperature drops while the temperature of the sensor plate remains at the initial value (ambient temperature). This temperature difference results in a heat flux from the plate towards the cooled gas. In the test time the pressure, hot-wire and heat flux measurements are performed.

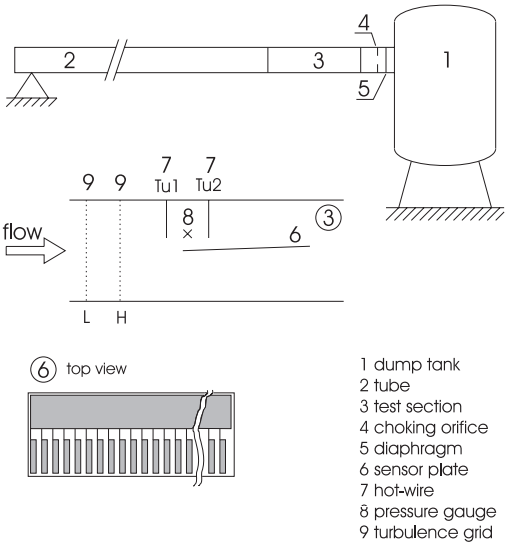

Fig. 1. Experimental set-up.

3. Pressure measurements

The Mach number is adjusted by the choking orifice. In an ideal Ludwieg tube, the Mach number is independent of the initial pressure in the test section. This means that the unit Reynolds number and the Mach number can be varied independently. Setting the initial pressure (and thus the initial density) determines the Reynolds number, while the geometry of the choking orifice determines the Mach number. By assuming an ideal gas and isentropic flow it is easy to derive a relation between the actual Mach number and the pressure ratio in the tube

$$M = \frac{2}{\gamma - 1}\left[\left(\frac{p}{p_i}\right)^{(-\gamma+1)/2\gamma} - 1\right], \tag{1}$$

where p_i is the initial pressure and p is the pressure recorded during an experiment. An example of a pressure signal is given in Fig. 2. A plateau in the signal is observed for about 40 ms, this is the time the Mach number at the test section is constant.

4. Heat transfer measurements

A thin film technique is used for measuring the temperature at the top of the sensor plate [15]. These sensors are made of titanium deposited on a substrate of glass. The sensor dimensions are: length: 3 mm, width: 20 μm and height: 200 nm. The first sensor is positioned 2 mm behind the leading edge while the distance between each sensor is 5 mm.

The sensor resistance is assumed to be a linear function of the temperature

$$R = R_0(1 + \alpha_0(T - T_0)). \tag{2}$$

Calibration gives the factor α_0 and R_0 for each sensor individually. The value of α_0 is approximately 2.2×10^{-3} K^{-1} and the value of R_0 is approximately 1 kΩ. Each sensor is part of a Wheatstone bridge. During an expansion experiment, the sensor voltage is recorded at a frequency of 50 kHz. The temperature then follows from Eq. (2). Heat fluxes at each streamwise position are calculated by numerically solving the one-dimensional

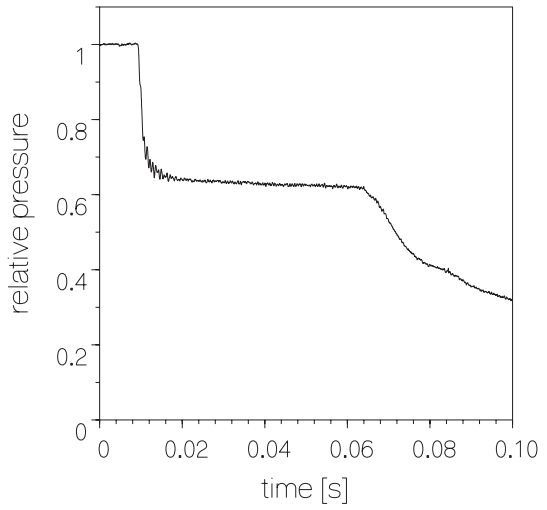

Fig. 2. Pressure signal, $M = 0.36$.

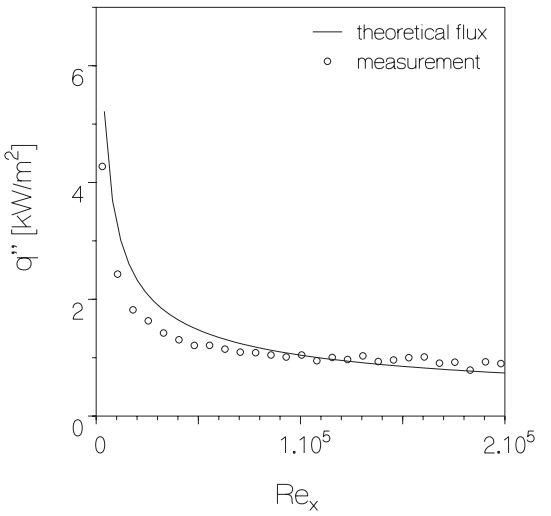

Fig. 3. Calibration experiment, $M = 0.36$, $Re_u = 1.5\times 10^6$ m^{-1}.

unsteady heat conduction equation perpendicular to the sensor plate

$$\rho c\frac{\partial T}{\partial t} = \frac{\partial}{\partial z}\left(k\frac{\partial T}{\partial z}\right), \tag{3}$$

with ρ, c and k the known substrate properties. Boundary conditions are the (measured) top temperature of the substrate and the bottom temperature which is assumed to be constant during an experiment. This assumption is valid as long as the thermal front does not reach the bottom side of the plate, which is true for 1 s after rupturing the membrane. As the complete experiment only takes 0.1 s, it is a valid boundary condition.

4.1. Heat flux calibration

To test the sensor accuracy, a laminar flow along the plate is initiated. The time mean heat flux should have the value expected from Blasius theory [16]

$$q_1''(x) = 0.332\frac{k}{x}(T_w - T_r)Re_x^{1/2}Pr^{1/3}, \tag{4}$$

where T_r is the recovery temperature which is a function of the Mach number.

Fig. 3 shows the measurements for a unit Reynolds number of 1.5×10^6 m^{-1} and a Mach number of 0.36. Also the expected heat flux is depicted. It is seen that there is a slight deviation for each sensor. This deviation is explained by three different error sources. The first one originates from calibration and dissipation effects in the sensors. A second deviation occurs when the boundary layer starts to develop not at the leading edge but at a virtual origin situated slightly earlier. In that case, the theoretical curve shifts towards the leading edge. The third error is introduced by a small pressure gradient. This is indicated by a systematic increase of the heat flux in streamwise direction. To avoid flow separation, the sensor plate has a small angle of attack (2.4°) which is the reason for this pressure gradient.

The data of each experiment are corrected for the above-mentioned deviations by estimating a multiplication factor. This factor is determined for all sensors separately by comparing the sensor output for a laminar flow to that for a theoretical Blasius flow.

5. Main stream turbulence

Turbulence in the flow is initiated by using turbulence generating grids. These grids can be positioned at two positions in front of the leading edge. Position 'H' is situated 167 mm upstream and position 'L' is situated 232 mm upstream. The grid dimensions, mesh and bar diameter, together with the turbulence levels (accuracy ±2%) obtained are given in Table 1.

Hot-wire measurements are performed to determine the main stream turbulence level. In the present set-up, a wire length of 0.6 mm and a diameter of 2.5 μm has been used. The wire is positioned 10 mm above the sensor plate, which is high enough to not disturb the boundary layer. The hot-wire is used at two streamwise positions. The first position ($Tu1$) is 27 mm in front of the leading edge of the sensor plate while the second position ($Tu2$) is 30 mm behind the leading edge. These positions were chosen for constructional reasons. The wire is calibrated for four different unit Reynolds numbers at each position. The sampling frequency was 400 kHz.

A typical hot-wire signal for the 4 mm turbulence grid is given in Fig. 4. The background turbulence level,

Table 1
Turbulence levels

Grid (–)	Re_u (m^{-1})	$Tu1$ (%)	$Tu2$ (%)	D (mm)	Mesh (mm)
4H	1.5×10^6	3.49	2.39	4	16
4L	2.4×10^6	2.65	2.42	4	16
3H	1.5×10^6	2.28	2.04	3	15
3L	2.4×10^6	2.16	1.93	3	15
2H	3.0×10^6	1.66	1.30	2	8
2L	4.0×10^6	1.37	1.22	2	8
1H	3.0×10^6	1.15	1.03	1	11.5
1L	5.0×10^6	1.25	0.95	1	11.5
–	–	0.25	0.25	–	–

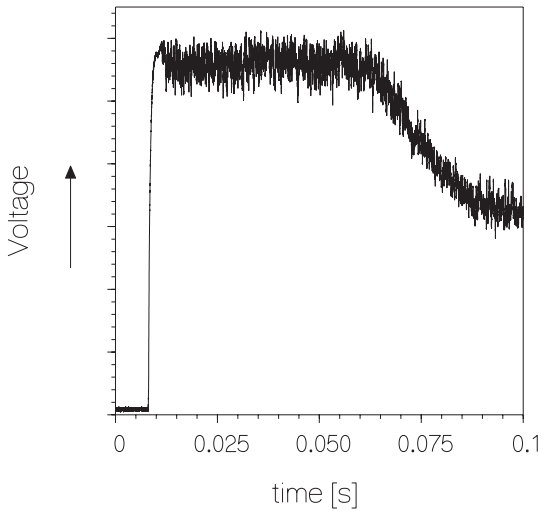

Fig. 4. Hot-wire signal, $M = 0.36$, grid: 4H, position: $Tu1$, $Re_u = 1.5 \times 10^6$ m^{-1}.

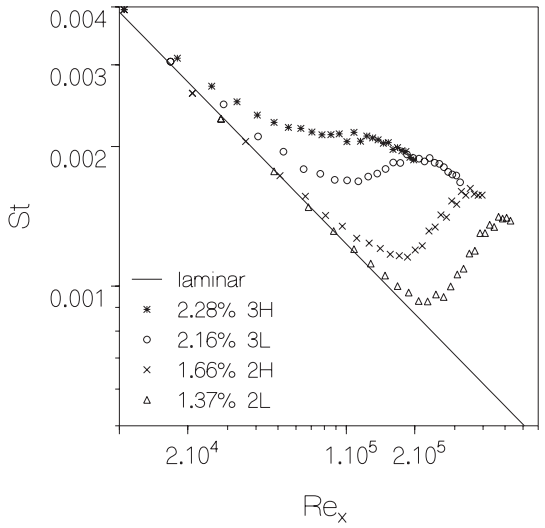

Fig. 5. Stanton number distributions for the 2 and 3 mm grid.

i.e. the turbulence level which is measured without a grid, is found to be 0.25%.

Several length scales are important in the transition process. Significant scales are the turbulence length scale and the boundary layer thickness. Due to the high velocity in the set-up, the boundary layer thickness is small. The length scale of the turbulence in our experiment can be characterised by the mesh size. Therefore, the ratio of the turbulence scale and the boundary layer thickness is large, indicating that the present measurements are performed in a new parameter range. Our experiments resemble the conditions in a gas turbine more, closely, compared to measurements in a low speed wind tunnel.

6. Transition experiments

Heat flux measurements are performed for the different turbulence generating grids at a Mach number of 0.36. The unit Reynolds number in the test section is adjusted such that the transition region covered a few centimetres of the plate (Table 1).

There are 27 sensors available on the sensor plate. However, the maximum number of channels which can be used in one experiment is 16. For this reason the heat flux measurements have to be performed twice. The first experiment is taken with the odd numbered sensors connected, while the second experiment is taken with the even numbered sensors. Afterwards both measurements are combined.

To compare the fluxes for several experiments, they are transformed to Stanton numbers

$$St = \frac{q''(x,t)}{(T_w - T_r)k\,Re_u\,Pr}. \tag{5}$$

The results are given in Figs. 5 and 6. The heat flux distributions are comparable to those of Blair [11] obtained for low main stream velocities (30 m/s). However,

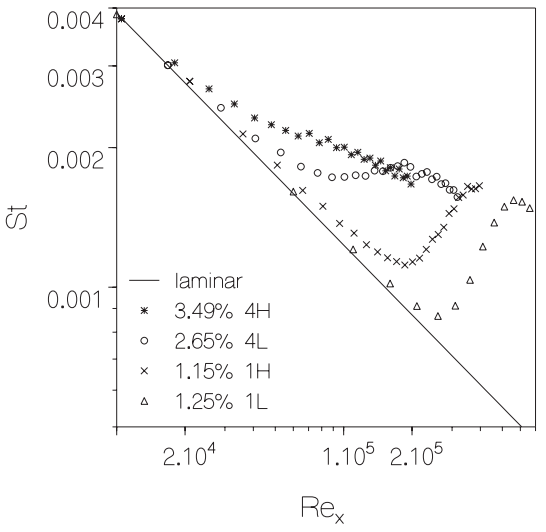

Fig. 6. Stanton number distributions for the 1 and 4 mm grid.

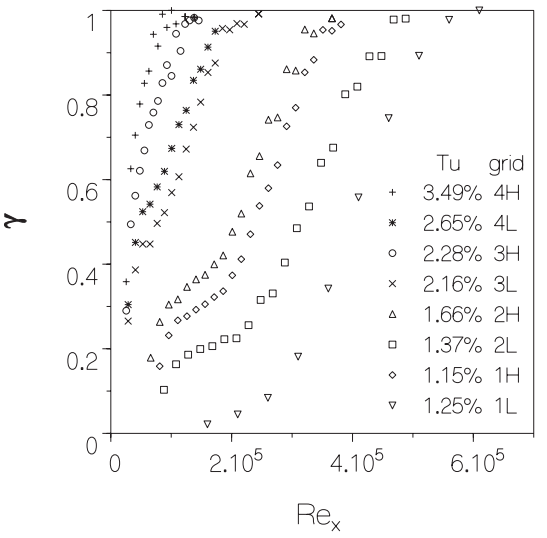

Fig. 7. Intermittency distributions for several grids.

the turbulence level giving a certain distribution is lower in our case (our 1.25% distribution is comparable to Blair's 2% distribution). This also was observed in earlier experiments [17]. It was found that increasing the Mach number results in a decrease of the turbulence level, while no influence on the transition was recognised (when the turbulence grid is unchanged). This indicates that the structure of turbulence has a more significant effect on transition than the turbulence level itself.

The intermittency γ at a certain streamwise position is defined as the fraction of time the flow is turbulent on that position. However, due to the fact that in our case heat flux measurements are performed, we used another manner to define the intermittency. From the theoretical laminar heat flux $(q_l(x))$ and a fitted curve through the turbulent part $(q_t(x))$, the intermittency is obtained

$$\gamma(x) = \frac{\overline{q(x)} - q_l(x)}{q_t(x) - q_l(x)}. \tag{6}$$

The mean heat flux $\overline{q(x)}$ is determined by taking the average of fluxes during the test time (which is 40 ms). This definition implies that transition starts when the heat flux starts to deviate from the laminar value.

Determining the intermittency by means of the friction coefficient was already done by Dhawan and Narasimha [5]. The heat flux analogy was proposed by Chen and Thyson [18]. This approach follows from the Reynolds analogy which describes that for a Blasius boundary layer, the friction coefficient and the heat flux are related by a factor of two.

The intermittency curves for the experiment with several turbulence generating grids are presented in Fig. 7.

6.1. Low turbulence levels

Models describing intermittency are based on the assumption that turbulent spots, discovered by Emmons [4], develop after a certain critical momentum thickness Reynolds number, $Re_{\theta,tr}$, has been reached. Dhawan and Narasimha [5] assume that spots originate with a Gaussian distribution around the transition start (x_{tr}). Added to the assumption that the spots form at an infinitesimal size at one streamwise position, the *Narasimha* model [6] is obtained. The Narasimha model assumes a constant spreading rate of the spot. This rate is characterised by a non-dimensional parameter σ, which depends on the spot growth angle β and the trailing and leading edge velocities of the turbulent spot

$$\sigma = U \tan(\beta)[U_{te}^{-1} - U_{le}^{-1}]. \tag{7}$$

If N is the number of spots per spanwise length, the change of intermittency at a certain streamwise position is characterised by

$$\frac{d\gamma}{dx} = N\sigma. \tag{8}$$

Johnson and Fashifar [7] stated that the change in number of spots is represented by

$$\frac{dN}{dx} = \frac{(1-\gamma)n}{U} - \frac{N^2\sigma}{(1-\gamma)}. \tag{9}$$

In this equation U is the mean velocity of the spots and n the number of spots per second per meter span which originate at the transition start. The first term on the right-hand side is the amount of turbulent spots which reach the present streamwise position by convection. Merging of spots is described by the second term and

gives a negative contribution to the number of spots. Eqs. (8) and (9) are combined to an ordinary differential equation describing the intermittency in streamwise direction

$$(1-\gamma)\frac{\mathrm{d}^2\gamma}{\mathrm{d}x^2}+\left(\frac{\mathrm{d}\gamma}{\mathrm{d}x}\right)^2-\frac{\sigma n}{U}(1-\gamma)^2=0. \tag{10}$$

From this equation the Narasimha intermittency distribution is obtained, when assuming $\sigma n/U$ to be constant

$$\gamma(x)=1-\exp\left(-\frac{\sigma n}{2U}(x-x_{\mathrm{tr}})^2\right). \tag{11}$$

Johnson and Fashifar [7] extended the model by taking $\sigma n/U$ not constant but a linear function of the streamwise distance. This results in the Johnson intermittency distribution (J is a constant)

$$\gamma(x)=1-\exp(-J(x-x_{\mathrm{tr}})^3). \tag{12}$$

It should be noted that a similar distribution (third-order dependence on the streamwise distance) was already proposed in the original paper of Emmons [4]. He obtained this distribution by assuming not a point wise (at x_{tr}) but a distributed (constant along x) breakdown of turbulent spots.

The start of boundary layer transition can be defined in several manners. The first definition is that the start of transition takes place when turbulent spots are initiated. These spots influence the heat transfer as well as the friction coefficient. So, the point where the heat transfer and/or the friction coefficient starts to deviate from the expected value in the laminar case is the transition start. The second definition used is that the start takes place at the point where the heat flux and/or the friction coefficient obtains a local minimum. The latter definition implies a start which is situated further downstream compared to the former definition. However, as is seen in Figs. 5 and 6, the latter definition is not applicable for turbulence grids with large diameter bars because a local minimum cannot be recognised.

To determine the start obeying the first definition, Narasimha [6] transformed the intermittency by

$$F(\gamma)=\sqrt[s]{-\ln(1-\gamma)}. \tag{13}$$

Transforming a real Narasimha intermittency distribution with $s=2$ results in a straight line. The start is obtained by taking $F(\gamma)=0$, while the transition length depends on the slope of F. The transformation with $s=3$ is used to see whether an intermittency obeys the Johnson model.

In Fig. 8 the intermittency distribution for the 1L grid is shown. Fig. 9 gives the function F for the experiment with the 1L grid. It is seen that the latter part of F indeed follows a line while the front part deviates. The discrepancy is explained by the fact that turbulent spots do not originate at one fixed streamwise position but in a small area around this position. The Johnson model gives a better description of the intermittency distribution for the 1L grid, especially for the transition start.

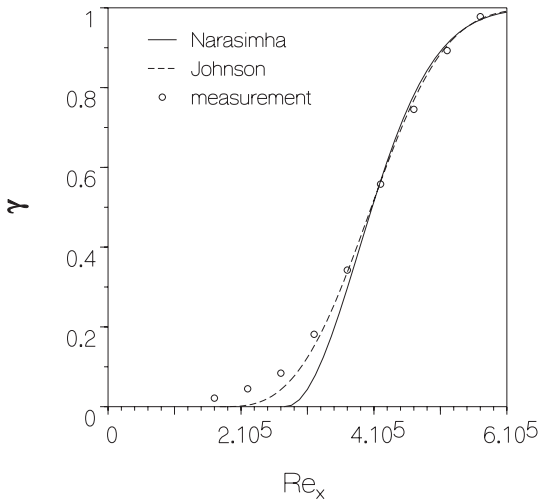

Fig. 8. Intermittency distribution for the 1L grid.

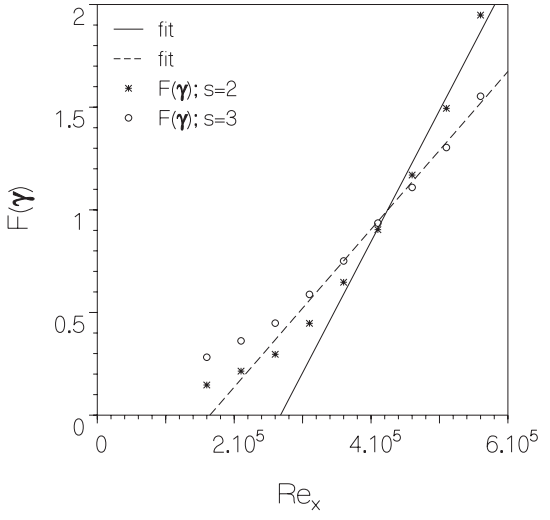

Fig. 9. Transformed intermittency distribution for the 1L grid.

6.2. Turbulent spots

Individual turbulent spots are recognised in the heat flux signals. The output for several sensors in the transition zone for the 2L grid are given in Fig. 10 (all sensor outputs are plotted on the same y-scale but shifted vertically; sampling frequency of the signals: 50 kHz). Clearly, turbulent spots are recognised. The spots grow

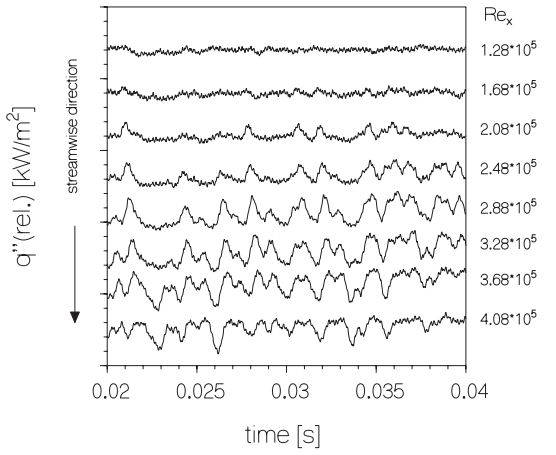

Fig. 10. Heat flux signals for several streamwise sensors for the 2L grid.

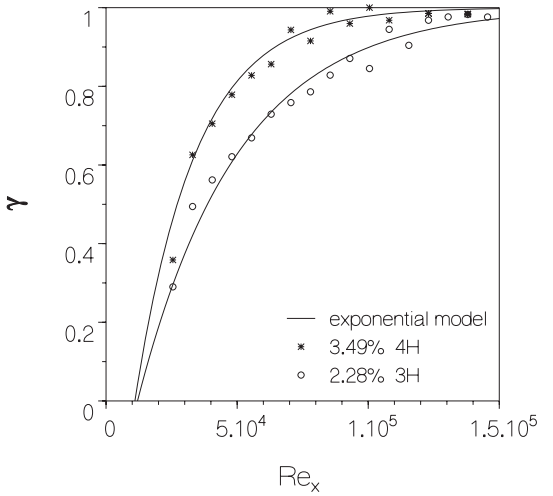

Fig. 11. Intermittency distribution for the 4H and 3H grid compared to the exponential model.

and convect in streamwise direction. Cross-correlation of the output (sampling frequency 380 kHz, peak distance determination inaccuracy ±2%) of two sensors, situated at $Re_x = 2.28 \times 10^5$ and $Re_x = 2.68 \times 10^5$, gives the mean velocity of the spots. The velocities taken relative to the main stream value are given in Table 2. All the correlation experiments are performed at a unit Reynolds number of 4×10^6 m^{-1}. The main cause for the spread is caused by a non-sharp cross-correlation. A peak is visible in the correlation diagrams, but determining the peak centre introduces the inaccuracy.

Clark et al. [12] performed measurements in an ILPT to determine the velocity of naturally occurring turbulent spots. They found that for a Mach number of 0.25 and 0.55, the mean velocity of the spots was 65% of the main stream velocity. Ching and La Graff [13] did experiments at several unit Reynolds numbers in an LICH. For a unit Reynolds number of 2.4×10^6 m^{-1}, they found a mean spot velocity of 68% and for a unit Reynolds number of 4.2×10^6 m^{-1} they found a velocity of 63%. Therefore, the values listed in Table 2 are slightly higher than the velocities which are found for natural occurring spots. No attempt has been made to distinguish between the leading- and trailing-edge velocities of the turbulent spots. In our case too many spots were present in the flow to determine these features.

Table 2
Mean spot velocities

Grid	Relative velocity (%)
1L	75
1H	80
2L	64
2H	74

6.3. High turbulence levels

The intermittency distributions for the 3H and 4H grids are depicted in Fig. 11. These distributions cannot be described well by either the Narasimha or the Johnson model. However, when another source of the spot production is used, better results are obtained. It is assumed that the turbulent spots are initiated not only at one streamwise position but along the whole distance in the transition region. So, this hypothesis is identical to the one proposed by Emmons [4]. Spots are assumed to enter the boundary layer at a rate of m per meter in streamwise direction per meter in spanwise direction (note that the dimension of m is different compared to that of n). A second assumption is that the spots enter the boundary layer with an initial size w. The boundary layer is intrinsically stable. Therefore the spots do not grow. The resulting equation for the streamwise intermittency is

$$\frac{d\gamma}{dx} = mw(1-\gamma), \tag{14}$$

which has an exponential distribution as solution

$$\gamma(x) = 1 - \exp(-mw(x - x_{tr})). \tag{15}$$

Fig. 11 shows the intermittencies for the 3H and the 4H grid. Good agreement is found for the exponential model. So, apparently the hypothesis of no spot growth in combination with a distributed spot production fits the measurements.

6.4. Intermediate turbulence levels

In measurements at intermediate turbulence levels, the results cannot be described by either of the preceding

models. However, it appears that the results can be described by a combination of models. Our hypothesis is that during the first part of transition, defined as the pre-transition part, spots are able to enter the boundary layer but decrease in size due to diffusion in the still stable boundary layer. After a certain Reynolds number the boundary layer will become unstable, spots start to grow and the conventional route to turbulence, according to the Narasimha model, is followed. It is likely that the spot growth parameter, or for present purpose: a spot decay parameter, is a function of the streamwise distance. However, for simplification this is not incorporated in the model. The equation describing the pre-transition zone with decreasing turbulent spot size is

$$\frac{\mathrm{d}\gamma}{\mathrm{d}x} = -a\gamma + mw(1-\gamma). \tag{16}$$

In this equation, the first term on the right-hand side describes the change in intermittency due to the decrease of spot size. For this purpose the parameter a, which is a measure for the 'spot decay rate', is introduced. The second term is the number of spots which enter the boundary layer. This term is the same as in the exponential model (Eq. (14)). The solution for the intermittency is

$$\gamma(x) = \frac{1}{1+(a/mw)}[1-\exp(-(mw+a)(x-x_{\mathrm{tr}}))]. \tag{17}$$

This pre-transition distribution has an exponential growth towards an intermittency which is not identical to one.

Fig. 12 shows the measurements together with the pre-transition model and the Narasimha model. It shows good agreement for the data obtained for the 2L, 2H and 3L grid. Therefore, the pre-transition model combined with the Narasimha model gives a good description of the intermittency distribution at these intermediate turbulence levels. It seems that until a certain Reynolds number is reached turbulent spots with a certain initial size enter the boundary layer and decrease in size. After this Reynolds number, which is dependent on the turbulence grid, the boundary layer seems to be unstable enough to allow the spots to grow and the Narasimha intermittency curve is followed. The same trend is found for the 1H grid (lower turbulence level). The only difference is that the latter part of the transition zone is described better by the Johnson model than by the Narasimha model. Both distributions are given in Fig. 13.

For the intermittencies which are described by the exponential and the pre-transition model, an estimate of the numerical value of the parameters involved can be made. A data fit gives the values of mw and a directly (Table 3).

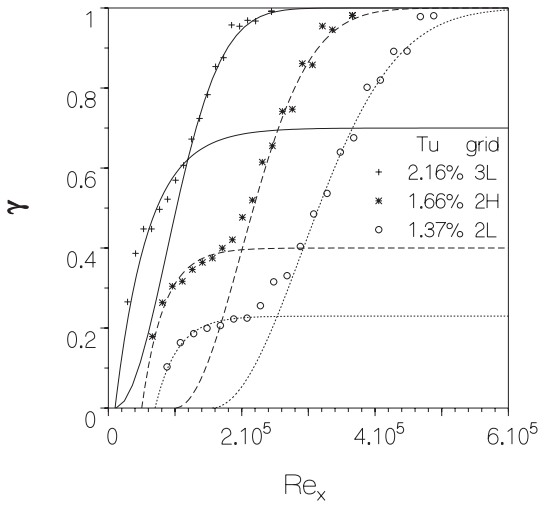

Fig. 12. Intermittency distributions for the 2L, 2H and 3L grid compared to the pre-transition model.

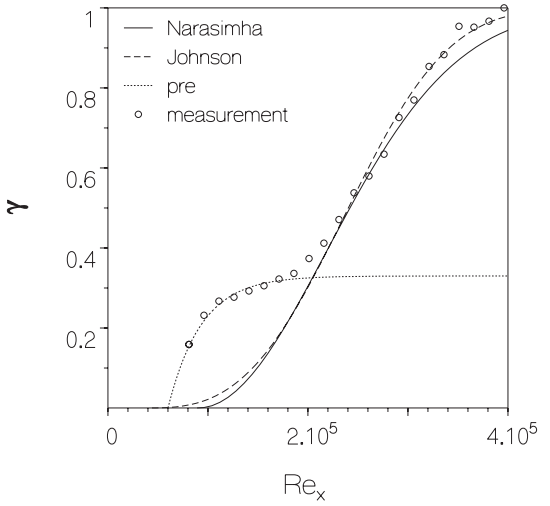

Fig. 13. Intermittency distribution for the 1H grid.

6.5. Pre-transition–Narasimha coupling

The Narasimha model can be transformed to a dimensionless form

$$\gamma(x) = 1-\exp(-\hat{n}\sigma(Re_{\mathrm{x}}-Re_{\mathrm{tr}})^2). \tag{18}$$

In this equation, $\hat{n}\sigma$ is the dimensionless spot production parameter which describes the transition length. Mayle presented a correlation for the spot production parameter as a function of the turbulence level

$$\hat{n}\sigma = 1.5\times 10^{-11}\,Tu^{7/4}. \tag{19}$$

Table 3
Parameter values

Grid (–)	mw (m^{-1})	a (m^{-1})
4H	65	–
3H	39	–
3L	34	82
2H	36	126
2L	28	92
1H	49	101

The data used for deriving this relation together with the spot production parameters resulting from the present measurements are given in Fig. 14. The production parameters are determined in the area in which the Narasimha model describes the intermittency best. The turbulence levels are measured 27 mm in front of the leading edge of the sensor plate. This implies that the turbulence level just above the leading edge is slightly lower. We find that $\hat{n}\sigma$ agrees well with that of Eq. (19).

Mayle also derived a correlation for the momentum thickness Reynolds number at transition start. This relation is given by

$$Re_{\theta,\mathrm{tr}} = 400\,Tu^{-5/8}. \tag{20}$$

The 1L grid is the only grid which does not show a pre-transition or exponential intermittency distribution. Determining the transition start by using Eq. (13) gives a $Re_{\theta,\mathrm{tr}}$ of 343. Using Mayle's equation gives an expected start at 348, so good agreement is found for this turbulence grid. However, the transition start for the other grids is situated much more towards the leading edge (Table 4; accuracy ±10%).

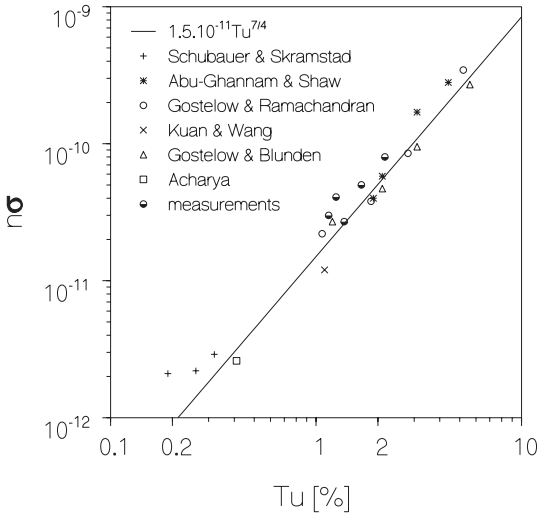

Fig. 14. Dimensionless spot parameter as a function of the turbulence level.

Table 4
Momentum thickness Reynolds number

Grid	$Re_{\theta,\mathrm{tr}}$
4H	70
4L	76
3H	73
3L	66
2H	148
2L	176
1H	163
1L	343

6.6. Cross-correlations

At low turbulence levels spots are recognised in the flux signal (e.g. Fig. 10). However, no spots are seen directly in the transition zone where the exponential model fits the measurements. The same is valid for the signals taken in the pre transition zone for the several grids. Cross-correlating the output of two sensors, with a streamwise distance of 10 mm, gives a correlation at a velocity of approximately 56% of the main stream velocity (sampling frequency 380 kHz; filtered at 50 kHz). This indicates that in these areas in the transition zone disturbances are present which move at a velocity which is characteristic for turbulent spots. This leads us to the conclusion that very tiny spots, which are not directly visible in the heat flux signals, are present in both transition cases. For completeness, also cross-correlation measurements are performed in the laminar boundary layer. For these experiments no correlation at any velocity was present, indicating that no artefacts are present.

An estimate of the initial spot size for the exponential and pre transition intermittency distributions can be made as follows. From the high frequency measured heat flux in the transition zone it is found that the (unfiltered) noise level is 2 kW/m^2. The sensor signal should raise from the laminar value to the turbulent value when the sensor (width 3 mm) is covered fully by a spot. In this case the sensor output increases with a flux level of the order of 1.5 kW/m^2, depending on the unit Reynolds number and the stream wise position. To detect spots with size in the order of the sensor width a minimum sampling frequency of 25 kHz is needed. For the correlation experiments the frequency was 380 kHz, so detection of that large spots should not be a problem.

Now suppose that the spotsize is $\frac{1}{3}$ of the sensor width. This corresponds to a flux increase of 0.5 kW/m^2 and a frequency of 75 kHz. As well as the noise level and sampling frequency are not sufficient to detect these spots. While no individual spots are recognisable in the flux signal but the cross-correlation indicates the appearance of spots, it is estimated that the sensor is

covered for less than $\frac{1}{3}$. Therefore, this estimation gives a maximum size of 1 mm (approximately 15 times the boundary layer thickness at the transition start). Note that this argument also holds for clusters of spots.

7. Conclusions

Boundary layer transition experiments are performed at high subsonic velocities. It is found that several stages in the transition process can be recognised, depending on the turbulence generating grid. These stages are well described by assuming some new sources of the initiation and growth of turbulent spots. Fig. 15 shows the three different intermittency distributions obtained in the present experiments. The observations in the heat flux signals as a function of the turbulence grid, can be summarised in five regions which are given below.

1. *Laminar boundary layer*. In this region no turbulent spots are recognised. Cross-correlation at high frequency does not give any indication of small spots.
2. *Transition zone for the 4H and 3H grids* (*high turbulence levels*). No turbulent spots can be recognised in the heat flux signals directly. However, cross-correlation of high frequency flux signals indicates that small spots are present. The exponential model describes the intermittency well.
3. *Pre-transition zone for the 1H, 2L, 2H and 3L grid* (*intermediate turbulence levels*). No turbulent spots are recognised in the heat flux signals directly. However, cross-correlation of high frequency flux signals indicates that small spots are present. The front part of the intermittency curve is described by an intermittency distribution which follows from the assumption that spots decrease in size.
4. *Transition zone for the 2L, 2H and 3L grid*. Turbulent spots can clearly be recognised in the heat flux signals. This zone is described well by the Narasimha intermittency distribution.
5. *Transition zone for the 1L grid*. Turbulent spots can clearly be recognised in the heat flux signals. This zone is described well by the Johnson intermittency distribution.

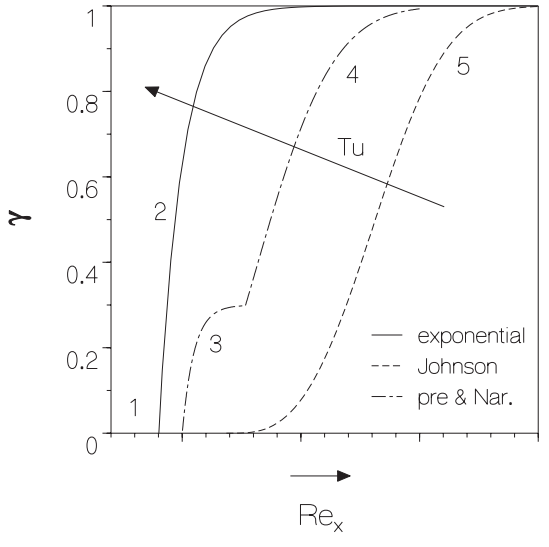

Fig. 15. Intermittency distributions for several models.

References

[1] R. Narasimha, The laminar–turbulent transition zone in the boundary layer, Prog. Aerospace Sci. 22 (1985) 29–80.
[2] R. Narasimha, Region of a boundary layer, J. Aero. Sci. 24 (1957) 711–712.
[3] R.E. Mayle, The role of laminar–turbulent transition in gas turbine engines, J. Turbomach. 113 (1991) 509–537.
[4] H.W. Emmons, The laminar turbulent transition in a boundary layer, J. Aero. Sci. 18 (1951) 490–498.
[5] S. Dhawan, R. Narasimha, Some properties of boundary layer flow during the transition from laminar to turbulent motion, J. Fluid Mech. 3 (1958) 418–436.
[6] R. Narasimha, On the distribution of intermittency in the transition region of a boundary layer, J. Aero. Sci. 24 (1957) 711–712.
[7] M.W. Johnson, A. Fashifar, Statistical properties of turbulent bursts in transitional boundary layers, Int. J. Heat Fluid Flow 15 (1994) 283–290.
[8] Y.S. Kachanov, Physical mechanisms of laminar boundary layer transition, Annu. Rev. Fluids Mech. 26 (1994) 411–482.
[9] B.J. Abu-Ghannam, R. Shaw, Natural transition of boundary layers – the effects of turbulence, pressure gradient and flow history, J. Mech. Engrg. Sci. 22 (1980) 213–228.
[10] R. Narasimha, K.J. Devasia, G. Gururani, M.A. Badri, Narayanan, Transitional intermittency in boundary layers subjected to pressure gradient, Exp. Fluids 2 (1984) 171–176.
[11] M.F. Blair, Influence of free-stream turbulence on turbulent boundary layer heat transfer and mean profile development, part 1 – experimental data, J. Heat Transfer 105 (1983) 33–40.
[12] J.P. Clark, T.V. Jones, J.E. La Graff, On the propagation of naturally-occurring turbulent spots, J. Engrg. Math 28 (1994) 1–19.
[13] C.Y. Ching, J.E. La Graff, Measurements of turbulent spot convection rates in a transitional boundary layer, Exp. Thermal Fluid Sci. 11 (1995) 52–60.
[14] H. Consigny, B.E. Richards, Short duration measurements of heat transfer rate to a gas turbine rotor blade, J. Engrg. Power 104 (1982) 542–551.
[15] Hogendoorn CJ. Heat transfer measurements in subsonic transitional boundary layers. Ph.D. thesis, Eindhoven University of Technology, 1997.
[16] Schlichting H. Boundary Layer Theory, seventh ed. McGraw-Hill, New York, 1979.

[17] Schook R, de Lange HC, van Steenhoven AA. Effects of compressibility and turbulence on bypass transition. ASME-Paper 98-GT-286, 1998.

[18] K.K. Chen, N.A. Thyson, Extension of Emmons' spot theory to flows on blunt bodies, AIAA J 9 (1971) 821–825.